The Minimum Dissipation State for Tokamaks

Cheng Zhang, Deng Zhou

Institute of Plasma Physics, Chinese Academy of Science, People's Republic of China
E-mail: czhang@mail.ipp.ac.cn and zhangc@fusion.gat.com

Abstract. The principle of minimum dissipation rate subject to helicity and energy balance is applied to tokamaks with an arbitrary aspect ratio. We solved the resulting Euler-Lagrange equations analytically and numerically. It is found that for low and general aspect ratio tokamaks, there exists different typical minimum dissipation state, corresponding to the typical experimental current profile respectively. It is also found that there exist different types of relaxed states in different regions of the parameter space for a selected device. Three forms of current profile are presented under different experimental conditions for a low aspect ratio tokamak like NSTX. The first peaks in the edge region of the high field side similar as the typical experimental form. The second peaks in the central region on the equatorial plane. The third may have a hole or reverse in the central part. $E_0/\eta B_0$ is the key parameter in determining the final relaxed state; both the second and the third states could be obtained violently by increasing it to be above a critical value.

1. Introduction

Experiments have shown that in most cases tokamak plasmas tend to evolve to a 'self- consistent' natural profile and under some conditions may evolve to other forms of states [1-3]. It implies that a relaxation mechanism may exist in tokamak plasmas. Since the Minimum Energy Principle developed by Taylor, many authors have employed variational principles to explain plasma relaxation states observed in experiments [4-13].

Taylor's theory has been widely employed in laboratory and astrophysics plasmas. It successfully predicted the features of reversed field pinch experiments. A number of other authors have applied the principle of minimum dissipation rate to driven steady state RFPs and predicted the current and magnetic profiles. Farengo *et al* presented the application of the same principle to tokamaks [10]. In their work the Ohmic dissipation was minimized under the conditions of energy balance, helicity balance, constant uniformly applied electric field and uniform ambient magnetic field. They used a simplified 1D model and gave analytical solutions to the resulting Euler-Lagrange equation.

In this paper, we apply the principle of minimum dissipation rate with the constraints of helicity and energy balance to an ohmically driven tokamak with an arbitrary aspect ratio. Different from that of Ref. [10], our model is intrinsically 2-dimensional. The applied electric field and the ambient toroidal magnetic field are assumed to be inversely proportional to the distance from the symmetric axis. The toroidal current profile from resulted Euler-Lagrange equation is resolved analytically. The self-consistent solutions of whole Euler-Lagrange equations as well as both helicity and energy balance equations are obtained numerically for a set of given parameters and boundary conditions. We find that the solutions give some different forms of current profiles for a typical low-aspect-ratio tokamak like NSTX and some of these forms are observed in experiments [15]. Each current profile mode is achieved by adjusting controllable parameters such as plasma resistivity, boundary toroidal magnetic field or boundary electric field. The key parameter in determining the final relaxed states is found. Our results also show that there exists the different typical current profile for low and general aspect ratio tokamaks.

2. Euler-Lagrange Equations and Their Solutions

The dissipation rate is minimized subject to helicity and energy balance. We introduce the functional

$$W = \int_V \eta j^2 d\tau + \lambda_0 \left[\int_V \eta \vec{j} \cdot \vec{B} d\tau - \int_V \vec{E} \cdot \vec{B} d\tau \right] + \beta_0 \left[\int_V \eta j^2 d\tau - \int_V \vec{E} \cdot \vec{j} d\tau \right] \qquad (1)$$

where λ_0 and β_0 are Lagrangian multipliers, η is the resistivity assumed uniform through the whole plasma. For stationary plasma, it is reasonable to assume that the applied electric field and the ambient toroidal magnetic field are inversely proportional to the distance from the symmetric axis. The cross section is assumed to be a rectangle. In the cylindrical coordinate system, as shown in FIG.1, taking the first variation and introducing $\lambda=\lambda_0/(1+\beta_0)$, $\beta=\beta_0/2(1+\beta_0)$, we finally obtain the Euler-Lagrange equations

$$\frac{1}{r}\frac{\partial}{\partial r}\left(r\frac{\partial j_\varphi}{\partial r} \right) + \frac{\partial^2 j_\varphi}{\partial z^2} - \frac{j_\varphi}{r^2} + \lambda^2 j_\varphi - \frac{\lambda^2}{2\eta} E_\varphi = 0 \qquad (2a)$$

$$\frac{1}{r}\frac{\partial}{\partial r}\left(r\frac{\partial B_\varphi}{\partial r} \right) + \frac{\partial^2 B_\varphi}{\partial z^2} - \frac{B_\varphi}{r^2} + \lambda j_\varphi - \frac{\lambda}{2\eta} E_\varphi = 0 \qquad (2b)$$

$$\frac{\partial}{\partial r}\left(\frac{1}{r}\frac{\partial \psi}{\partial r} \right) + \frac{1}{r}\frac{\partial^2 \psi}{\partial z^2} + j_\varphi = 0 \qquad (2c)$$

and the following boundary condition (3), where $B_0=B_\varphi(r_0)$, $E_0 = E_\varphi(r_0)$ and $r_0 = R_0$.

$$j_{\varphi b} = \frac{1}{r_b}\left(\beta E_0 r_0 + \frac{\lambda B_0 r_0}{2} \right) \qquad (3)$$

The analytical solution for Equ. (2a) [12,13] is presented as $j_\varphi = Y + E_0 r_0 / 2\eta r$ (4)
where Y is the solution of the homogenous equation related to (2a) [11], with boundary condition

$$Y_b = \frac{1}{r_b}\left(\beta E_0 r_0 - \frac{E_0 r_0}{2\eta} + \frac{\lambda B_0 r_0}{2} \right) = \frac{a(\beta,\lambda) r_0}{r_b} \qquad (5)$$

We have the solution of Y as $Y=Y_1+Y_2$ (6).
For $k^1_n \le \lambda < k^1_{n+1}$,

$$Y_1 = \sum_{m=1}^{n} \frac{a_m J_1(k^1_m r)}{\sin(u_m h)} \left[\sin(u_m z) + \sin(u_m (h-z)) \right] + \sum_{m=n+1}^{\infty} \frac{a_m J_1(k^1_m r)}{\sin(u_m h)} \left[\sinh(u_m h) + \sinh(u_m (h-z)) \right]$$

with $u_m^2 = \lambda^2 - (k^1_m)^2$ for $1 \le m \le n$ and $u_m^2 = (k^1_m)^2 - \lambda^2$ for $m > n$. $k^1_m = x^1_m / r_{00}$, x^1_m is the m^{th} zero point of the Bessel function of order 1. For $\nu_m \le \beta < \nu_{m+1}$ with $\nu_n = n\pi / h$,

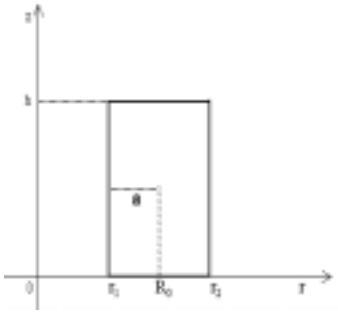

Fig. 1. Coordinate system

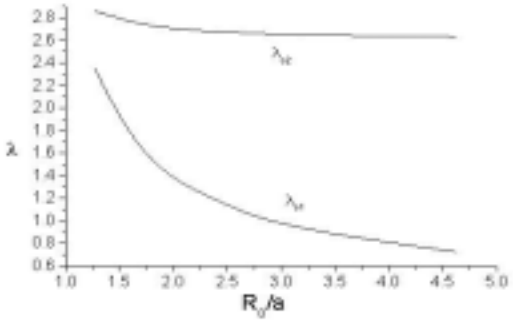

Fig. 2.The dependence of λ_{c1} and λ_{c2} on aspect ratio

$$Y_2 = \sum_{n=1}^{m}[c_n J_1(k_n r) + d_n N_1(k_n r)]\sin(v_n z) + \sum_{n=m+1}^{\infty}[c_n I_1(k_n r) + d_n K_1(k_n r)]\sin(v_n z)$$

where J_1, N_1, I_1 and K_1 are respectively Bessel and modified Bessel functions. Coefficients a_m, c_n and d_n are obtained by applying the boundary conditions. The analytical analyses indicate that for a device of given dimensions, Y is only related to $\alpha(\beta,\lambda)$ and λ; λ determines the form of Y as the analysis in ref. [11], while $\alpha(\beta,\lambda)$ determines its magnitude. The final current profile is determined by Lagrange multiplier λ, as well as the relative magnitude of two terms in (4). For given E_0/η and B_0, the values of α and λ should be obtained consistently by energy and helicity balance conditions. The self-consistent solutions of whole Euler-Lagrange equations as well as both helicity and energy balance equations are obtained numerically.

3. Main Results

3.1. Difference of typical relaxed state between low and general aspect ratio tokamaks

It is found that for a device of given geometric parameters, there exists a critical value λ_{c2}. For λ lower than λ_{c2}, the form of Y changes from a decreasing function of r continuously to a function with a maximum in the center on the equatorial plane as λ increases up to a value larger than λ_{c1}. But when λ is larger than λ_{c2}, Y is reversed in the central part. Fig.2 shows the dependence of λ_{c1} and λ_{c2} on the aspect ratio with a fixed cross section of a = 0.67m, h = 2.7m. We find that the region between λ_{c1} and λ_{c2} is getting smaller as aspect ratio decreases, and becomes a very narrow region for a low aspect tokamak. Meanwhile, for a low aspect ratio tokamak, though Y may have a peak in the central part for $\lambda_{c1}<\lambda<\lambda_{c2}$, the second part on the right side of Eq. (4) is always dominant, therefore the total current on equatorial plane is always a decreasing function of r. FIG.3 shows the typical current profile with λ lower than λ_{c2} from our numerical calculation for NSTX-like tokamak (R_0 = 0.85 m, a = 0.67m, h = 2.7m[14]). It is similar with the typical experimental result [15]. For a large aspect ratio tokamak, however, the second part of Eq. (4) is

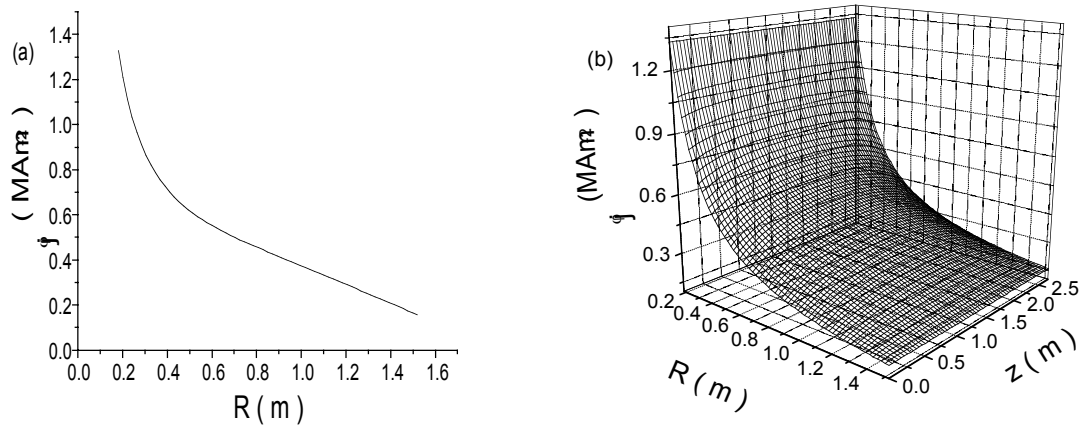

FIG. 3. Toroidal current on equatorial plane (a) and in minor cross section (b) for a low λ .
Parameters are $B_0 = 0.29\,T$, E_0/η =0.38, $\lambda = 2.0$, $\alpha = 0.1$

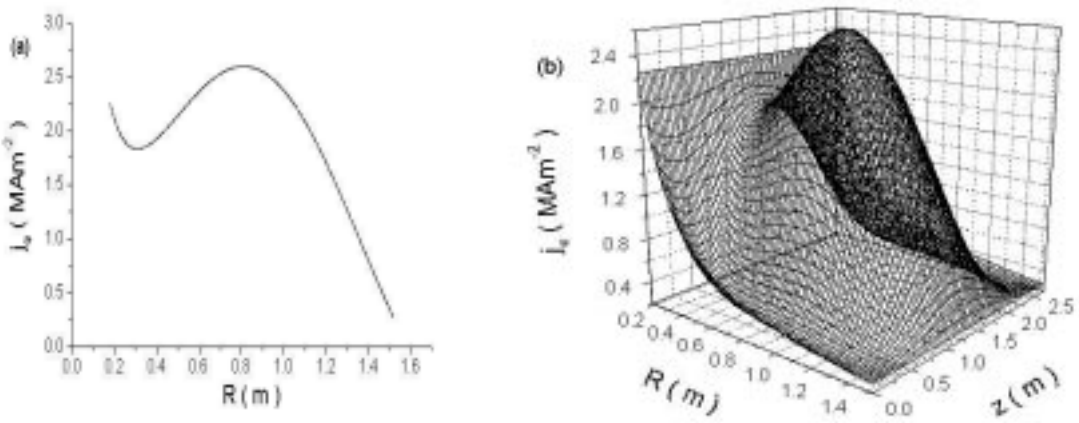

FIG. 4. Toroidal current on equatorial plane (a) and in minor cross section (b) for a high λ . Parameters are B_0=0.266 T, E_0/η =1.694, α = -0.371, λ=3.8.

almost uniform, therefore we can obtain a typical current profile with an extremum in the central region for $\lambda < \lambda_{c2}$, which corresponds to the typical experimental form for general tokamak.

3.2.Three forms of current profile for a low aspect ratio tokamak

Three forms of current profile are presented under different experimental conditions for a low aspect ratio tokamak like NSTX. The first as the typical experimental form peaks in the edge region of the high field side as shown in Fig.3. There exist two other possible types, which could be transformed violently from the first when λ increases to a value higher than λ_{c2} (2.86 for NSTX-like). One type is for a negative α value, where the current peaks in the central region, as shown in FIG.4. The other one for a positive α value, where the current may have a hole as shown in FIG.5 or reverse in the central part for other parameters. Each current profile mode is achieved by adjusting controllable parameters such as plasma resistivity, boundary toroidal magnetic field or electric field.

3.4. Key parameter in determining the final relaxed state

It is found that the boundary parameter $(E/\eta B)_b$, or $E_0/(\eta B_0)$ for our model, is a key parameter in determining the final relaxed state. Only when it is larger than a critical value, $E_0/(\eta B_0)$~5.8m^{-1} for NSTX-like, can we obtain solutions with λ larger than critical value λ_{c2}. Both the second and the third types could be obtained violently by increasing $E_0/(\eta B_0)$ to be above its critical value. The rapid transformation from the typical current profile to a central peak form has been observed in the experiment with a high loop voltage on NSTX [15], which seems to agree with our results.

4. Conclusion and discussion

The minimum dissipation principle subject to energy and helicity balance is employed to determine the plasma current profile of a tokamak with an arbitrary aspect ratio. The resulting

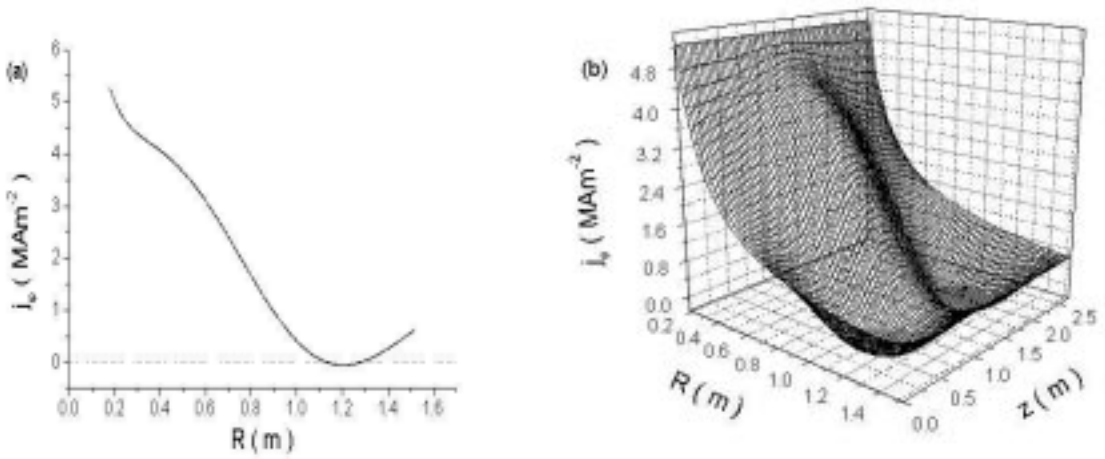

FIG.5. Toroidal current on equatorial plane (a) and in minor cross section (b) for a high λ *.*
Parameters are $B_0 = 0.266$ *T,* $E_0/\eta = 1.8$, $\alpha = 0.212$, $\lambda = 4.85$.

Euler-Lagrange equations were solved analytically and numerically. It is found that for low and general aspect ratio tokamaks, there exists different typical minimum dissipation state, corresponding to the typical experimental current profile respectively. It is also found that there exist different types of relaxed states in different regions of the parameter space for a selected device. Three forms of current profile are presented under different experimental conditions for a low aspect ratio tokamak like NSTX. The first, as a typical mode, peaks in the edge region of the high field side similar as the typical experimental profile [15]. The second peaks in central region on the equatorial plane. The third may have a hole or reverse in the central part. $E_0/(\eta B_0)$ is the key parameter in determining the final relaxed states. Both the second and the third states could be obtained violently by increasing $E_0/(\eta B_0)$ to be above a critical value. It is expected that the typical state could transfer to other states. Especially when $E_0/(\eta B_0)$ is close to the critical value, the current profile may be modified rapidly by MHD perturbation event, similar as that observed in experiment [15].

[1] KADOMTSEV, B. B., Tokamak Plasma: A Complex Physical System, (1992).
[2] FUJITA, T., et al, Phys. Rev. Lett. 87 (2001) 245001.
[3] HAWKES, N. C., et al, Phys. Rev. Lett. 87 (2001) 115001.
[4] TAYLOR, J. B., Phys. Rev. Lett. 33 (1974) 1939.
[5] TAYLOR, J. B. Rev. Mod. Phys. 58 (1986) 741.
[6] HAMEIRI, E., et al, Phys. Rev. A 35 (1987) 768.
[7] MONTGOMERY, D. and PHILLIPS, L., Phys. Rev. A 38 (1988) 2935.
[8] WANG, C. Y. ,et al, Phys. Fluids B 3 (1991) 3462.
[9] BEVIR, M. K., et al, Plasma Phys. Control. Fusion 34 (1993) 133.
[10] FARENGO, R. et al, Plasma Phys. Control. Fusion 36 (1994) 465.
[11] ZHANG, Cheng, et al, Nucl. Fusion 41 (11) p1567, Nov. (2001).
[12] ZHANG, Cheng, et al, 43rd APS-DPP Meeting, [UP1/056], Long Beach, California (2001).
[13] ZHOU, Deng and ZHANG, Cheng, Plasma Sci. Tech. 4 (2002) 1147.
[14] MENARD, J. E., et al, Nucl. Fusion 41 (2001) 1197.
[15] MENARD, J. E., 41st ASP-DPP Meeting, Seattle (1999).